CHAPTER II
THEORETICAL BACKGROUND AND LITERATURE REVIEW

2.1 Liquid Crystalline Polymer (LCP)

A liquid crystal refers to a matter that exhibits properties between those of a conventional liquid and those of a solid crystal. For instance, a liquid crystal may flow like a liquid, but its molecules may be oriented in a crystal-like way. When the liquid crystal is formed from the isotropic state some amount of positional or orientational order is gained (Brown *et al.*, 1969). It is this order that accounts for the anisotropies of the substance. Liquid crystalline polymers (LCPs) consist of repeating stiff mesogenic units (liquid crystalline monomer units that are incorporated either in the main-chain or in the side chain of a polymer backbone). The molecules which form liquid crystals are anisotropic, i.e. either rod-like (calamitic) or disklike (discotic). Liquid crystals form certain characteristic phases, e.g. nemetic, smectic and cholestoric. The nematic liquid crystal has a high degree of long range orientational order but no long-range positional order (Fig. 2.1).

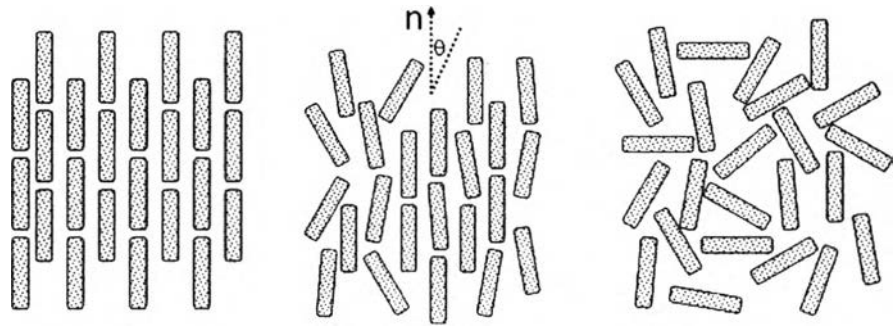

Figure 2.1 Schematic diagram showing molecular order in the LCP (from left to right; crystal, nematic, isotropic)

When liquid crystalline (LC) materials are heated, the molecules may undergo several different mesophase transitions before an isotropic liquid is obtained. The LC behavior can exist in two forms, i.e. lyotropic and thermotropic. In the former case, the LC behavior occurs when the LC mesogen is dissolved in a

solvent above a certain critical concentration. For thermotropic materials, the LC phenomenon occurs in the melt phase and depends on the temperature.

2.2 Binary LCP/ Thermoplastic Blends

Thermotropic liquid crystalline polymers (LCPs) are remarkably high performance thermoplastics that exhibit high modulus, high strength, high toughness, good creep resistance, and low coefficients of thermal expansion. The unique features of these polymers are their low shear viscosity in the nematic molten state and their high molecular alignment in the solid state after thermoplastic processing. These distinctive properties arise from their stiff linear molecular structure, which makes them readily align themselves to the flow direction. The incorporation of an LCP as a minor phase into a typical thermoplastic may offer the potential of improved melt processibility (Brostow *et al.*, 1996; Broston *et al.*, 1996). In addition, due to the intrinsically high modulus of the LCP phase, the mechanical properties of the blends could be enhanced. Not only does a rigid rod LCP generally form separate domains when blended with a typical thermoplastic, these domains also elongate into fine fibrils and reinforce the matrix under proper processing conditions and blend compositions, giving rise to the name 'in-situ composites' (Kiss, 1987). Blends of commercial LCP with a wide variety of thermoplastics, e.g. polypropylene (PP), polyamide 6 (PA6), polycarbonate (PC), polyethylene terephthalate (PET), polybutylene terephthalate (PBT), and poly(ether ether ketone) (PEEK) have been widely investigated over the past decades. These blends were fabricated by conventional compounding techniques, i.e. extrusion or injection (Tjong, 2003). Figure 2.2 shows the successful formation of poly(ether imide)/ Rodrun LC-5000 in-situ composites (Bastida *et al.*, 2000).

Table 2.1 summarizes reinforcing modes for thermoplastic polymers. It is clear that thermoplastics can be reinforced macroscopically by incorporating fibers such as carbon fiber, glass fiber, and aramid fiber (Kevlar) having diameters of 1 to 10 μm. To achieve a high-modulus and high-strength composite, a higher percentage of fiber content (up to 30%, 45%, and even 60%) is required. Another mode of reinforcing thermoplastics occurs at the molecular level by the presence of rigid rod-

like molecules of microfibrils like those of lyotropic liquid crystalline polymers. The individual fiber can have a diameter of as low as 0.5 nm, although the final fiber diameters in the resulting composite can become 10–30 nm. Young's modulus of molecular composites increases significantly upon the addition of as little as 5 wt% of the reinforcing agents. The in-situ composites fall in the in middle category – the microscopic reinforcing mode – as the reinforcing LCP fibrils can have the diameters of approximately submicrometer order of magnitude. It should be noted that the larger the aspect ratio (L/D ratio) of the fibrils, the more pronounced the reinforcing effect. Factors that influence LCP fibrillation in a thermoplastic matrix include the LCP characteristics, LCP content and processing conditions.

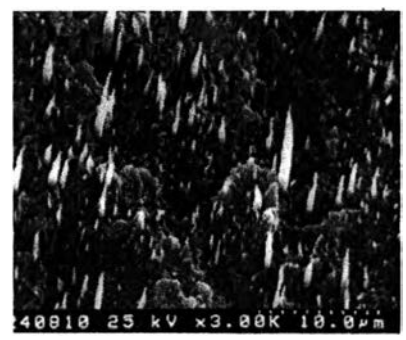

Figure 2.2 The binary blend of poly(ether imide)/ Rodrun LC-5000.

The key factor that has been reported to provide good LCP fibrillation is the low viscosity ratio (the LCP phase to the matrix) of near or less than one. shown in Table 2.2 is the study done by Lusignea *et al.* (1999). They reported the morphology of 10 wt% LCP dispersed in a thermoplastic of various types. It is evident from their results that a viscosity ratio less than unity does not guarantee for LCP fibrillation. Beery has demonstrated the importance of the interfacial tension between the two phases which also plays a vital role on the blend morphology (Beery and Siegmann, 1991). The combined effects of viscosity, interfacial tension, and shear rate may be represented by the capillary number, Ca, expressed as

$$Ca = \frac{\eta_m \dot{\gamma}}{\sigma / R} = \frac{\tau}{\sigma / R} \qquad (2.1)$$

where η_m is the matrix viscosity, $\dot{\gamma}$ the shear rate, R the LCP droplet radius ($R = D/2$), σ the interfacial tension of polymer pairs, and τ the shear stress.

Table 2.1 Reinforcing modes for thermoplastic polymers (Chung, 2001)

Reinforcing mode	Macroscopic	Microscopic	Molecular
Reinforcement	Monofilament	Microfibril	Rigid-rod molecules
Diameter	10 μm	0.01 μm	0.5 nm
Materials	FRP (Fiber reinforced plastics)	In situ composite	MC (Molecular composites)

Table 2.2 Morphology of dispersed LCP phase (LCP/matrix, 10/90, by weight), related to viscosity ratios (number in parentheses) of LCP to matrices (at a shear rate of 57.6 s^{-1}) (Lusignea *et al.*, 1999)

Matrix	Extrusion Temperature (°C)				
	270	300	320	340	360
PBT	Spheres (6.9)				
PC	Deformed spheres (0.32)	Spheres (0.16)	Spheres (0.13)		
PES		Fibrils (0.0095)	Fibrils (0.0075)	Fibrils (0.0058)	
PSF			Fibrils (0.0096)	Fibrils (0.0041)	Fibrils (<0.0041)

According to Taylor (Taylor, 1932), the capillary number is the ratio of the two opposing forces, i.e. the viscous forces that tend to deform the droplet to the counteracting interfacial forces that tend to resist the deformation and keep the droplet shape spherical. As a result, the shear stress must be adjusted to be larger than half of the interfacial energy (σ / D) to obtain an efficient fibrillation. One of the simplest way to do so is to select the proper processing temperature that the matrix polymer exhibits greater viscosity than the LCP. Examples have been shown by Kalkar *et al.* (2007), and Tan *et al.* (2002), who utilized such concept and studied the resulting mechanical performance of the blends. Those works were conducted on the systems with a viscosity ratio less than one while this research focused on the systems with a greater viscosity ratio to evaluate how effective this approach would be in providing LCP/ thermoplastic blends with promising mechanical properties.

Most commercial LCPs are incompatible with thermoplastics, leading to the lower-than-expected mechanical performance of the LCP/thermoplastic blends (Tjong, 2003). Fiber pullout is the principal mechanism responsible for the failure of incompatible LCP/thermoplastic blends. Poor interfacial adhesion remains a chief barrier in achieving high performance in situ composites. Thus, suitable compatibilizer additions might be necessary for the improvement of the interfacial adhesion of the blend components. The properties of LCP/PP and LCP/PA6 blends compatibilized with PP functionalized by maleic anhydride (MA-g-PP) are well documented in the literature (Seo *et al.* 1999; Tjong *et al.*, 2000; Zeng *et al.* 2003). One of the popular commercial LCPs used is Vectra A950 manufactured by Ticona. Its chemical structure is shown is Figure 2.3.

The reaction scheme accounting for the compatibilizing effects of MA-g-PP to PP/Vectra A950 blends was proposed as shown in Figure 2.4 (Seo *et al.*, 1997). O'Donnell and Baird suggested that interaction such as hydrogen bonding was also responsible for the compatibilizing effect of MA-g-PP on the LCP/PP blends [14]. Recently, Rath and coworkers used polyphosphazine as a compatibilizer for PEEK/Vectra A950 (VA) blends, taking the advantage of miscibility of polyphosphazine with PEEK and with VA. They observed an increase in the elongation as well as enhanced modulus and strength.

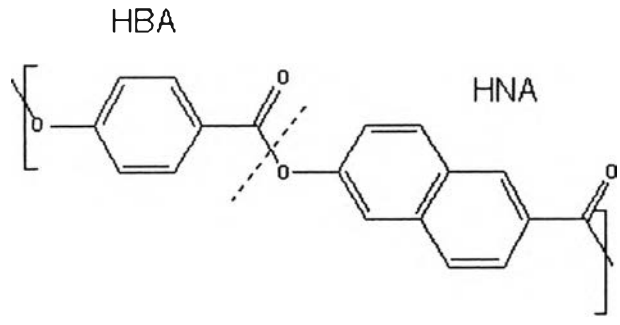

Figure 2.3 The chemical structure of Vectra A950, a liquid crystal copolyester of 73 mol % p-hydroxybenzoic acid (HBA) and 27 mol % 2-hydroxy-6-napthoic acid (HNA).

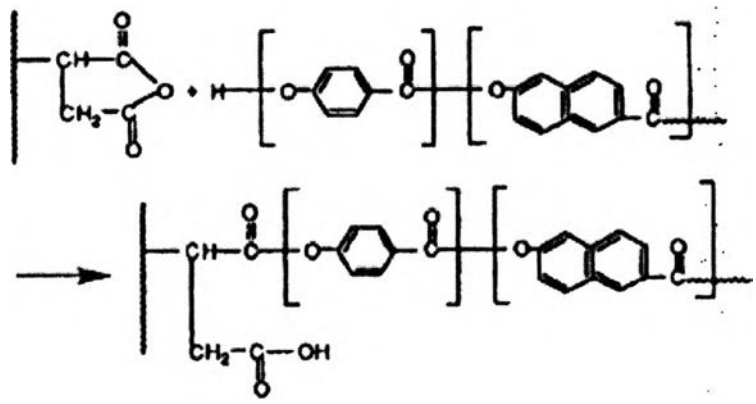

Figure 2.4 The chemical reaction between MA-g-PP and VA.

Poly(n-methylene terephthalates) are semicrystalline polymers whose rate of crystallization is strongly influenced by the number of methylene units in the alkylene moiety of the polymer (Gilbert and Hybart, 1972). PET, with two methylene units, is well known to crystallize very slowly (Brydson, 1989). Therefore it can be quenched into a highly amorphous state. The slow crystallization behavior is extremely useful when making PET beverage bottles and films where transparency and clarity are important. On the other hand, the slow crystallizing PET is unsuitable for engineering thermoplastic injection molding because it requires long molding cycle times unless it is nucleated. PBT, which has four methylene groups in its chemical repeating unit, crystallizes extremely fast. This makes it suitable for injection molding when a fast cycle time is needed. Because of the fast

crystallization rate and the high crystallinity achieved during molding, PBT has a higher heat distortion temperature than PET despite having a lower glass transition temperature. However, the extremely fast crystallization rate causes excessive mold shrinkage and results in warped surfaces in PBT articles with large flat surfaces (Brydson, 1989). Thus, the crystallization behavior of polyesters plays an important role in their end-use applications. Chuah (2001) reported that the isothermal crystallization rate of PTT was between those of PET and PBT when compared at the same degree of undercooling. Their results were in contrast to what previously reported, e.g. aromatic polyesters with odd numbers of methylene units were more difficult to crystallize than the even-numbered polyesters. Hence, PTT did not fit in the prediction and did not follow the odd-even effect.

Study of polymer crystallization under non-isothermal conditions is important based on the fact that most practical processing techniques proceed under non-isothermal conditions rather than isothermal conditions. For a long time, the non-isothermal crystallization of polymers has been investigated by many researchers. Although the process of non-isothermal crystallization of slowly crystallizing materials, like polymers, is relatively complex, it is very attractive to describe it using rather simple models. One of the methods commonly applied for the analysis of non-isothermal crystallization kinetic data was proposed by Ozawa (1971) and Jeziorny (1978) who extended the Avrami equation (Avrami, 1939; Avrami, 1940), which is applicable to the isothermal system, to fit the non-isothermal case by assuming that the sample was cooled with a constant rate from the molten state.

The Ozawa equation is expressed as follows:

$$1 - C(T) = \exp\left[-\frac{K(T)}{\phi_m}\right] \tag{2.2}$$

where $C(T)$ is the relative degree of crystallinity at temperature T, $K(T)$ is the crystallization rate constant, ϕ is the cooling rate, and m is the Ozawa exponent relating to the mechanism of nucleation and dimension of crystal growth. The double-logarithmic form of Eq. (2.2) is:

$$\ln\left[-\ln(1/C(T)\right] = \ln K(T) - m\ln\phi \tag{2.3}$$

If a linear relationship is achieved when $\ln[-\ln(1-C(T)]$ is plotted against $\ln\phi$, the Ozawa equation is then satisfactory in describing the non-isothermal crystallization process of that particular system. The Ozawa rate constant, $K(T)$, could be calculated from the anti-natural logarithmic value of the y-intercept, and the Ozawa exponent m is the slope. Hue and coworkers reported that the Ozawa equation can explain the non-isothermal crystallization of pure PTT but not the PTT/clay nanocomposites (Hu and Lesser, 2004). In the case of PET, it is shown that this model describes the non-isothermal process only at relatively low cooling rates. At rates exceeding 20°C/min, crystallization progress becomes higher, indicating higher crystallization rates than those resulting from the Ozawa approach. Additional deviation from the Ozawa model observed at the very beginning and the end of crystallization can be attributed to spatial constraints of spherulitic growth (Sajkiewicz *et al.*, 2001). Possible failure observed when utilizing Ozawa model might arise from the fact that non-isothermal crystallization is a dynamic process in which the crystallization rate is no longer constant but a function of time and cooling rate, the comparison in Ozawa analysis is to be carried out on experimental data representing widely varying physical states of the system, while these differences have not been taken into account in the model (Li *et al.*, 2006).

2.3 In-situ Hybrid Composites

The term in-situ hybrid composites were generally referred to LCP/ thermoplastic blends filled with inorganic reinforcement (He *et al.*,1997; He *et al.* 2000). Much work has been published on various types of reinforcements, such as glass fibers (Pisharath and Wong, 2003; Garcia *et al.*, 2003), carbon black (Shumsky *et al.*, 1993; Tchoudakov *et al.*, 2004), whisker (Tjong and Meng, 1999; Shumsky *et al.* 2000) and silica (Lee *et al.*, 2002; Lee *et al.*, 2003). Nano-size particulates filled polymers (nanocomposites) are of great interest due to their lower density, excellent performances and attractive prospect, compared to conventionally filled polymers (Rong *et al.*, 2001; Ray and Okamoto, 2003). Nano-size fillers such as carbon black (CB) and nano-SiO_2 have been reported to have unique influence on the morphology

of immiscible blends such as phase inversion, especially in conductive materials (Gubbels *et al.*, 1998; Steinmann *et al.*, 2002). Recently, it has been reported that nano-fillers such as nano-SiO_2 and nano-clay can also act as a compatibilizer in immiscible blends during mixing process (Voulgaris and Petridis, 2002; Wang *et al.*,2003; Khatua *et al.*, 2004; Ray *et al.*, 2004; Vermant *et al.*,2004; Zhang *et al.*, 2004; Ray and Bousmina, 2005). Hu *et al.*, (2003) introduced nano-size fumed silica of different surface properties into the LCP/polypropylene (PP) in-situ blends and found that hydrophobic nano-SiO_2 could efficiently promote the fibrillation of LCP droplets. Nano-clay acted as a compatibilizer in PA6/LCP blends (Zhang *et al.*, 2005), promoting the LCP fibrillation, and nano-SiO_2 did so by inhibiting the transesterification (Wu *et al.*, 2006). In these studies, the interfacial effects produced by the nano-filler during melt processing have been emphasized. Different to the nanometer-scale fillers, micrometer-scale or larger fillers rarely act as interfacial modifiers, but rather change the flow field in quantity resulting in the change in LCP fibrillation in in-situ hybrid composites (J.Chen *et al.*, 2006). For instance, glass beads were reported to improve LCP fibrillation in polycarbonate, due to the local shear prevailing between the neighboring beads (P.Chen *et al.*, 2006) On the other hand, when the stacked glass fibers were used in either PC or PA6 matrix, the LCP fibrillation was facilitated by the elongation flow developed through the microcapillary (Zheng *et al.*, 2003; Zheng *et al.*, 2004). Similar extensional flow was created by the microrollers of the rotating glass beads in PC (P.Chen *et al.*, 2005; P.Chen *et al.*, 2006) and PA6 (Ding *et al.*, 2004). It is clear that the flow field can be changed from shear flow to elongational flow in quality by fillers. So, introducing the filler particle will cause the extra hydrodynamic effects in in situ hybrid composites containing LCP droplets. Realizing the significant influences of inorganic fillers on the structure and performance of in-situ composites, two types of filler were chosen for study: the first one is zinc oxide particles (see 2.3.1) and the second one is multi-walled carbon nanotubes (CNTs) (see 2.3.2)

2.3.1 Zinc Oxide (ZnO)

Zinc oxide is a transition metal oxide occurring naturally as mineral zincite in the form of white powder. It is an amphoteric oxide, nearly insoluble in water and alcohol, but soluble in (degraded by) most acids, such as hydrochloric acid. It has three forms of crystal structure: hexagonal wurtzite, cubic zincblende and the hardly found, cubic rocksalt. The wurtzite is the most common form as it is stable at ambient conditions and thus was chosen for this study. Figure 2.5 illustrates unit cell of ZnO wurtzite crystals having zinc atoms in the tetrahedral sites and lattic parameters $a = 3.25$ *Å* and $c = 5.20$ *Å*. The wurtzite crystal structure is named after the mineral wurtzite and is an example of a hexagonal system.

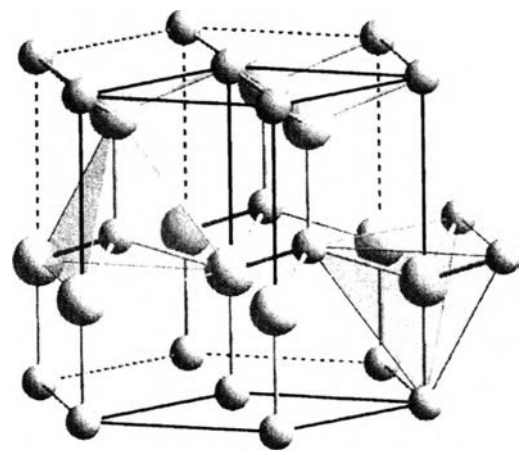

Figure 2.5 The wurtzite structure of ZnO (smaller spheres : zinc atoms, larger sphere: oxygen atoms).

Different synthesis methods have been developed to synthesize ZnO, especially in the nano-meter scale. These methods include microemulsion synthesis (Singhal *et al.*, 1997), sol-gel technique (Mondelaers *et al.*, 2002; Tokumoto *et al.*, 2003), mechanochemical processing (Tsuzuki *et al.*, 2001), spray pyrolysis and drying (Park and Kang, 1997; Okuyama and Lenggoro, 2003), thermal decomposition of organic precursor (Rataboul *et al.*, 2002), RF plasma synthesis (Sato *et al.*, 2003), supercritical-water processing (Viswanathan *et al.*, 2003), self assembling (Koh *et al.*, 2004), hydrothermal processing (Liu and Zeng, 2003; Zhang *et al.*, 2004), vapor transport process (Yu *et al.*, 2005), sonochemical or microwave-

assisted synthesis (Hu *et al.*, 2004), direct precipitation (Wang and Gao, 2003) and homogeneous precipitation. When most of the synthetic routes involve toxic chemicals, high temperature, and long reaction time, the microwave-assisted synthesis method is a rapid process, mild conditions and generates a product with high purity. Microwave heating has found a number of applications in chemistry. The ZnO particles can be synthesized by means of a domestic microwave oven in an aqueous system. Hence, this preparation method has the advantage of simplicity, short preparation time, inexpensiveness, low toxicity of the chemicals involved, and there is no requirement for post-annealing treatment. The successful formation of ZnO nanoparticles and ZnO nano-fibers by microwave-assisted synthesis has already been reported by several authors (Hamedani and Farzaneh, 2006; Takahashi, 2007).

Up to now there has been no research that utilized metal oxides to improve the properties of in-situ composites. Among the metal oxides, ZnO particles have received great attentions because of their good catalytic, electrical, electronic and optical properties as well as their low cost and extensive applications in diverse areas (Liang *et al.*, 2003; Sato *et al.*, 2003; Yang *et al.*, 2004). ZnO has also been studied as fillers of a series of polymers such as polyacrylonitrile (Tang *et al.*, 2003; Chae and Kim, 2006), polystyrene (Ma *et al.*, 2006), polystyrenebutylacrylate (Xiong *et al.*, 2003), polyphenylene sulfide (Bahadur and Sunkara, 2005) and PTFE (Li *et al.*, 2002). However, the extent of property modification depends on the base polymer and on the size, distribution and dispersion of the particles and on the adhesion at the filler matrix interface. Previous studies on polycarbonate/ZnO blends have demonstrated that PC filled with 0.5 wt% ZnO presented a higher modulus and similar tensile strength compared to neat PC, with a 74% reduction in the elongation at break. A ZnO concentration of 1 wt % dramatically reduced both the tensile strength and the elongation at break of PC. At 0.5 wt% loading of ZnO in the polycarbonate composites, results showed an increased hardness and reduced wear rate with respect to the neat PC both under pin-on-disk and under thrust-washer contact conditions (Carrion *et al.*, 2007). Also, a study done by Moustaghfir *et al.* (2004) proved that coating PC with ZnO can decrease the rate of oxidation and the rate of photo-yellowing of PC under solar UV light. In the meantime, as zinc oxide particles have a higher thermal conductivity as well as a greater heat capacity value

than polyacrylate, they absorb the heat transmitted from the surroundings and retard the direct thermal impact to the polymer backbone (Yang *et al.* 2002).

Polyesters are well-known to undergo acidolysis by acid end groups and alcoholysis by hydroxyl-end groups. They can undergo tranesterification (inter-chain ester-ester interchange) with itself or with other polyesters at high temperatures. The most dominant reaction to be found in high molecular weight polyesters and their blends is the tranesterification since the amount of the end-groups are relatively low, yielding much less significant acidolysis or alcoholysis. The tranesterification can have dramatic effects on the polymer properties such as the reduction of the molecular weight. As stated earlier, the greatest obstacle to achieve the in-situ composites with excellent mechanical properties is probably the poor compatibility between the polymer matrix and the LCP. It was then proposed by several researchers the concept of in situ compatibilization. This approach may involve the transesterification provided that the system contains ester exchange reactive groups. The products obtained are the copolymers locating at the polymer interfaces and thus reduce the interfacial tension. This results in a better adhesion between the LCP domains and the matrix which leads to a more effective stress transfer at the interface. Successful examples are Vectra A950/ polycarbonate (PC) blends and Vectra B950/ PET. Coltelli *et al.* (2008) made a comparison between the weaker nucleophilic ZnO and the stronger nucleophilic zinc acetate ($ZnAc_2$) on their catalytic reactivity for a tranesterfication between dibutyl maleate functionalized poly(ethylene) (POF) and PET and they observed that strong nucleophilicity leads to PET degradation since the strong nucleophilic catalyst tends to undergo substitution reaction with PET. These authors reported the presence of a certain amount of PET-POF copolymer without the detectable degradation of PET by the use of a ZnO catalyst. The aim to improve the performance of in-situ composites by the use of a third component filler in combination of the previous report on the role of ZnO as a tranesterification catalyst then became the motivation for the study of VA950/ PET/ ZnO in-situ hybrid composites.

2.3.2 Multi-Walled Carbon Nanotube (CNT)

The discovery of carbon nanotubes has drawn the huge interest from people in industry and academia. This is actually a direct consequence of the synthesis of buckminsterfullerene, C60, and other fullerenes, in 1985. The invention of the other stable, ordered structure form of carbon other than graphite and diamond encouraged scientists worldwide to search for other new forms of carbon. It was in 1991, that the Japanese scientist Sumio Iijima discovered fullerene-related carbon nanotubes. The nanotubes consisted of at least two layers, often many more, and ranged in outer diameter from about 3 nm to 30 nm. They were closed at both ends and could have a length-to-diameter ratio as large as 28,000,000:1. The chemical bonding of nanotubes is composed entirely of sp^2 bonds, similar to those of graphite. This kind of bonding provides the molecules with much higher strength than those composed of the sp^3 bonds found in diamonds. Nanotubes naturally align themselves into "ropes" held together by Van der Waals forces. They exhibit novel properties useful in many applications in nanotechnology, electronics, optics and other fields of materials science, as well as potential uses in architectural fields. They show extraordinary strength, unique electrical properties, and excellent thermal conductivity. Their final usage, however, may be limited by their potential toxicity and limited availability. The carbon nanotubes can be classified into single-walled and multi-walled nanotubes (see Fig. 2.6).

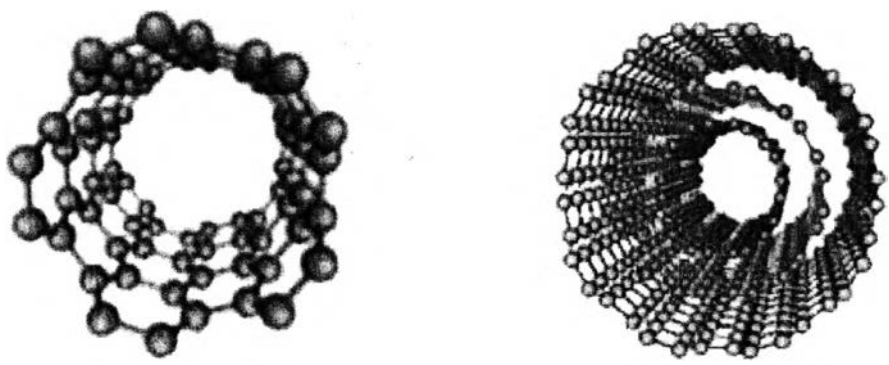

(a) (b)

Figure 2.6 The single-walled structure (a) and multi-walled structure (b) of carbon nanotubes.

The structure of a single-walled carbon nanotube can be conceptualized by wrapping a one-atom-thick layer of graphite called graphene into a seamless cylinder. The electrical properties of this kind of nanotubes are far superior to the multi-walled structure; however, nowadays the cost of production is still too high for commercial purposes. On the other hand, multi-walled nanotubes can be synthesized at a much cheaper cost. Their structure consists of multiple layers of graphite rolled in on themselves to form a tube shape, with an interlayer distance close to the distance between graphene layers in graphite, approximately 3.3 Å. The use of multi-walled carbon nanotubes as a conducting filler to produce advanced polymer nanocomposites is acceptable in terms of the cost and the properties acquired can be impressive, especially for electrically dissipative or conductive composite materials. The large aspect ratio of the nanotubes provides not only the unique electrical properties but also excellent mechanical properties. Owing to the theoretically extreme low percolation threshold (the critical filler volume fraction at which the sample resistivity drops down considerably as a result of filler particles being in contact with each other, see Fig. 2.7) caused by this very high aspect ratio, only small amounts of CNT is needed to achieve electrical percolation.

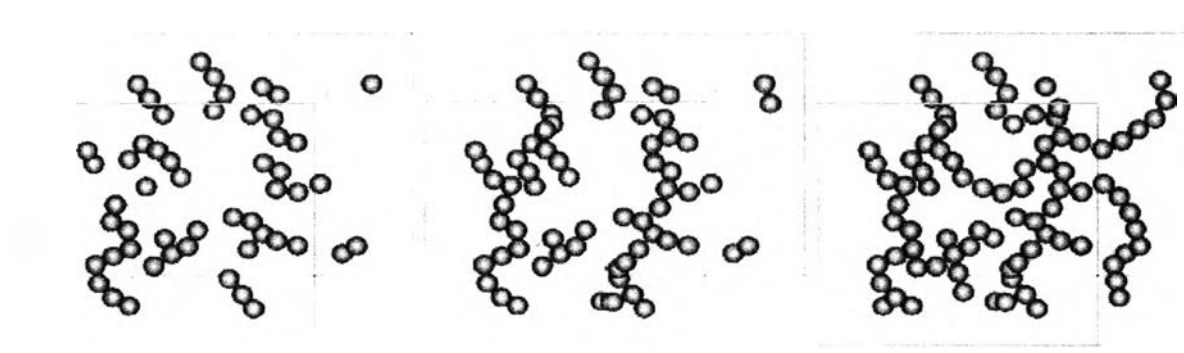

(a) (b) (c)

Figure 2.7 Schematic illustration of critical volume fraction in the percolative network of spherical inclusions in the random distribution: a) without percolation; b) critical volume fraction percolative network; c) percolative network cluster (Formulan and Souza, 1999).

Potschke *et al.* (2004 and 2007) published a number of studies regarding PC/CNT nanocomposites. He found that the electrical percolation threshold can be obtained at as low as 1 wt% CNT loading (see Fig. 2.8) as shown by a point at which a sudden rise of the electrical conductivity is observed. The conductivity increases only slightly with further increases in the filler concentrations.

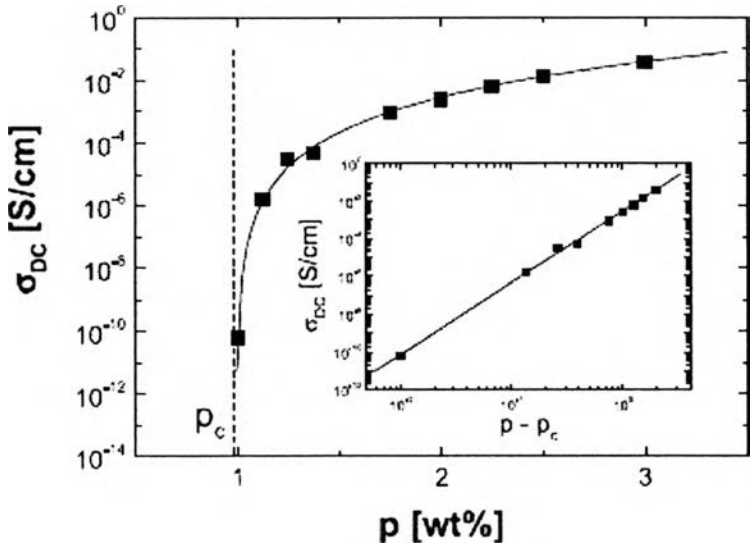

Figure 2.8 DC conductivity σ_{DC} versus nanotube concentration p for composites above the percolation threshold.

The combination of the carbon nanotubes and the liquid crystalline polymer has been studied by several researchers. Park *et al.* (2008) demonstrated that the use of a very small amount of carboxylated multi-walled carbon nanotubes (0.2 wt% or less) can promote the mechanical properties while retain the good processibility characteristics of an LCP. Kim et al. (2009) claimed that the thermal stability of the LCP nanocomposites was improved and they observed an increase in the storage and loss moduli in the presence of the acid-modified nanotubes (1.5 wt%) especially at low frequencies. The non-terminal behavior indicated the nanotube-nanotube and LCP-nanotube interactions. The uniform dispersion of nanotubes and the interfacial adhesion between the LCP matrix and the nanotubes were claimed to be crucial for the mechanical, thermal and rheological properties of the nanocomposites. Research works related to the electrical conductivity of the LCP

composites are limited. Among them, there are two interesting works that investigated the electrical conductivity of the electrically conductive blends containing an LCP, a thermoplastic matix, and a conductive filler; the work by Tchudakov *et al.* (2004) dealed with ternary blends of high impact polystyrene/ LCP/ carbon black; the other work was done by Mukherjee et al. (2010) claiming that the use of acid-modified multi-walled carbon nanotubes could enhance the thermal stability, and the storage modulus of the PC/LCP blends. They also reported the electrical percolation threshold of the systems to be between 1 and 3 wt%, close to that of the pristine PC (2 wt%).

2.3 Double Percolation

A significant reduction in the critical conductive filler volume fraction for electrical percolation can be achieved by utilizing the concept of double percolation through the formation of a co-continuous morphology in filled immiscible polymer blends. The basis of this concept requires two structural continuities; one is the continuous structure of the conductive fillers forming electrically conductive pathways and the other is the continuity of the phase in which these filler particles resides. The concept was first demonstrated by Sumita *et al.* (1991) in carbon black-filled immiscible blends. In this study, the selective localization of carbon black particles in a continuous phase along with the network formation of the particles themselves allowed the formation of electrical conductive pathways at a much smaller carbon black loadings. Since then, the double percolation concept has applied to many blend systems involving a variety of conductive fillers e.g., carbon black (Sumita *et al.*, 1991; Ibarra-Gomez *et al.*, 2003; Al-Saleh and Sundararaj, 2008), graphite nanosheets (Chen *et al.*, 2007), graphite (Thongruang *et al.*, 2002), carbon fibers (Wu and Shaw, 2004; Jin and Lee, 2007), and CNTs. (Potschke *et al.*, 2004; Wu and Shaw, 2006; Li *et al.*, 2007; Potschke *et al.*, 2007; Bose *et al.*, 2008; Li and Shimizu, 2008).

To describe the preferential localization of the conductive fillers observed from the experimental results, a thermodynamic parameter, namely, the wetting coefficient (ω_{12}) has been frequently used. The wetting coefficient or equivalent equations that can be used to predict the location of fillers is usually explained by the differences in interfacial energies between the fillers and the polymer components. Such differences arise form the dissimilarities in their polarities and surface energies. ω_{12} can be defined as;

$$\omega_{12} = \frac{\gamma_{s-2} - \gamma_{s-1}}{\gamma_{12}} \qquad (2.4)$$

where γ refers to the interfacial energy, the subscripts 1, and 2 refer to each polymer component, and the subscript s refers to filler particles. The particle will accumulate at the interface if $|\omega_{12}| < 1$ corresponding to $|\gamma_{s-2} - \gamma_{s-1}| < \gamma_{12}$. On the other hand, if $|\omega_{12}| > 1$ that is $|\gamma_{s-2} - \gamma_{s-1}| > \gamma_{12}$ then the fillers will be localized in one of the two phases.

Although the experimental data on the interfacial tensions between two polymers may be available, it is almost impossible to find the experimental data of the polymer/filler interfacial tensions, and thus they must be estimated from the theoretical models, e.g. Owens-Wednt, Girifalco-Good, or Wu equations. The discrepancies among these models can be significant but the localization of the fillers was successfully predicted in a number of studies.

Apart from the thermodynamic effect, the kinetic control also plays a vital role in determining the final morphology of the system. Since most molten polymers appear as viscous liquids, the state of filler dispersion and distribution inside the blends are not immediately attained. If the system is quenched before reaching its equilibrium, the final morphology may not agree with results predicted by thermodynamic control. This means that the filler may be found in the polymer with less viscosity even though the said polymer does not exhibit the better affinity according to the thermodynamic prediction. In general, the solid particles may migrate to the polymer that melts first regardless of the interfacial energy. Then if the mixing time is long enough, the particles will shows the tendency to transfer to the second molten polymer that provides a better affinity to them. Gubbels *et al.* (1998)

propose that the migration of filler particles from one phase to another is slower when the filler particles are originally confined in the more viscous phase Persson and Bertilsson (1998) hypothesized that the kinetic effects are weak and dominate only when the difference in interactions between each pair of polymer/filler is small. Further experiments done by Clarke *et al.* (2001) and Zhou *et al.* (2007) led to their argument that the thermodynamic control would dominate only when the viscosity ratio of both polymer phase is close to one. Up to this point, it may be concluded that one can produce the desired non-equilibrium morphologies by simply taking the advantage of this kinetic effects through the control of mixing rate and mixing sequences.

The double percolation concept has been used to the carbon-nanotubes filled polymer blends in order to acquire the attractive electrical conductivity. The nanotubes were found to be confined in the more polar phase, PC (Potschke *et al.*, 2003; Potschke *et al.*, 2007), PET (Wu and Shaw, 2004), or polyamide (Meincke *et al.*, 2004). Goldel *et al.* (2009) reported the shift of the electrical percolation threshold in the blends of PC/SAN/multi-walled carbon nanotubes to a lower nanotubes content compared to the nanotubes coorporating in the SAN alone. Their electrical percolation threshold of the ternary blends was found to be less than 1 wt% nanotubes loading compared to the 2 wt% found in nanotubes/PC and nanotubes/SAN (see Fig. 2.9). The co-continuous morphology is depicted in the two-dimensional TEM images as shown in Fig. 2.10. The dark areas represent the PC phase indicating the confinement of the nanotubes within PC domains alone. Even though the authors predispersed the nanotube in SAN prior to melting and the mixing time was only 5 min, the complete transfer of the nanotubes to PC was successful agreeing with the prediction from thermodynamic control. The difference between the interfacial energy of PC/CNT and SAN/CNT is only marginal and the wetting coefficient favors the localization of nanotubes in PC. The authors further confirmed the hypothesis proposed by Krasovitski and Marmur (2005) that unlike the spherical particles, for a high aspect ratio filler, only a small difference in wetting behavior is needed for complete penetration into the better wetting liquid. The localization of the nanotubes at the interface of the polymers is not stable and the driving force retains until the nanotubes totally penetrate into the PC phase that the system can reach its

equilibrium state. Nanotubes can accumulate on the polymer interface only when they align parallel to the interface.

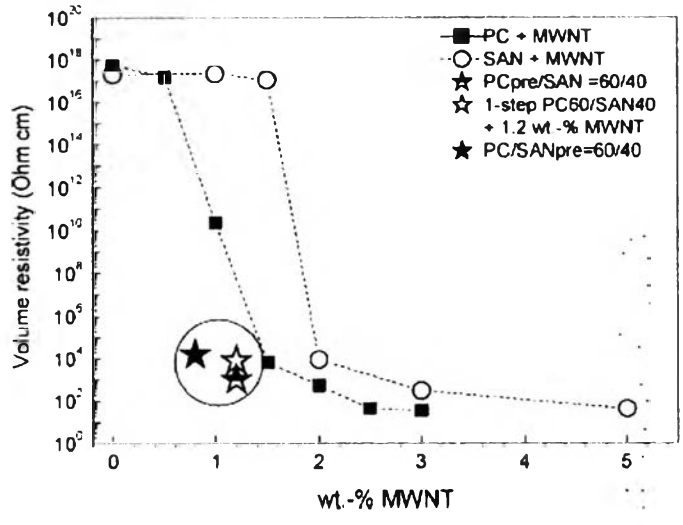

Figure 2.9 Volume resistivities of the investigated PC/SAN/CNT composites (stars in circle) and those of the single polymer composites PC-CNT and SAN-CNT (dashed lines).

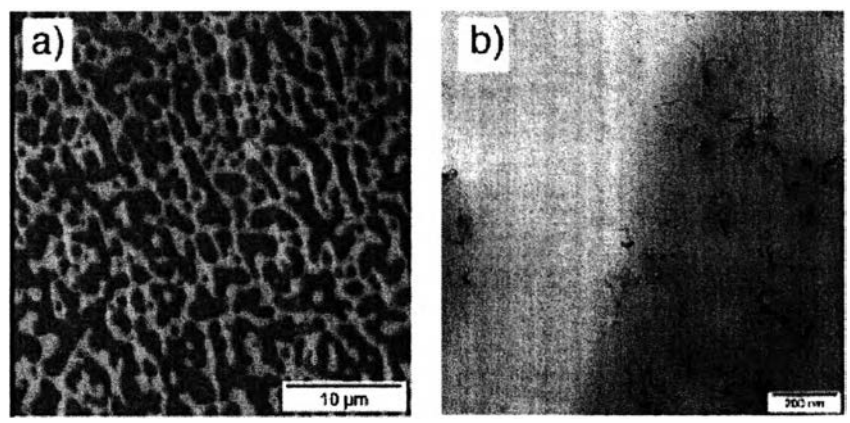

Figure 2.10 Transmission electron micrographs of the blends prepared by pre-compounding of 2 wt% CNTs in PC, subsequent blending with SAN: $(PC\text{-}CNT)_{60}/SAN_{40}$, 1.2 wt% CNTs in the blend: a) low magnification; b) high magnification.

2.4 Microwave Heating of Polymers

A dielectric material is an electrical insulator mostly with a resistivity higher than 10^9 ohm-cm. This criterion covers most polymeric material. When a dielectric material is brought into in an electric field that alternates at high frequency, heat is generated inside the material. This is known as heating by dielectric hysteresis or, in short, dielectric heating. Dielectric or radio frequency heating and microwave heating are both applications of this principle and thus are considered close cousins. Dielectric or radio frequency energy occupies the electromagnetic frequency spectrum of approximately 10 to 100 MHz whereas the microwave energy occupies 1000 to 100000 MHz. For industrial applications, the two most important microwave frequencies are 915 MHz and 2450 MHz. When a dielectric material is placed in a microwave field, the dipolar molecules will try to align their dipole moment along the field intensity vector which varies sinusoidally with time. As the direction of the vector reverses every half cycle, the polar molecules will try to re-align themselves accordingly. As a result, some of the microwave energy is lost in order to overcome the resulting internal friction. This results in a conversion of a portion of the microwave energy into thermal energy such that the generated heat is proportional to the number of reversal of electric field vectors, i.e. the frequency. The amount of displacement occurring during each reversal is determined by the electric field strength and hence the produced heat is also a function of the electric field strength just like radio frequency heating. The amount of heating depends on the field strength, frequency, and the material properties as reflected in the loss factor ($\varepsilon' \tan\delta$, see Eq. 2.5). To determine the rate at which electrical energy can be dissipated in a dielectric per unit volume, Q, the same equation used in dielectric heating can be applied to microwave heating as well.

$$Q = 2\pi E^2 f \varepsilon_0 \varepsilon' \tan\delta \qquad (2.5)$$

where f is the electric field frequency, E the electric field strength, ε_0 absolute permittivity of free space (8.854E-12 F/m), ε' relative permittivity or dielectric constant of the material, and $\tan\delta$ the loss tangent or dissipation factor.

Principally, with either microwave or radio frequency heating, heat is generated throughout the mass of material which is considered superior to conductive heating for polymers as they tend to have low thermal conductivity. Unlike conductive heating, microwave heating results in a highest temperature at the center and the lowest at the wall while the conductive heating does the opposite. Non-polar polymer such as polyethylene will not heat well by microwave heating unless filled with a microwave absorbing additive. The microwave welding is one of the modern techniques of joining polymers and their composites and may require the help of some additives for example, multi-walled carbon nanotube (Makeiff and Huber, 2006; Wang *et al.*, 2007), carbon black (Harper *et al.*, 2005), zinc oxide (Harper *et al.*, 2005), and talc (Harper *et al.*, 2005). In the literature, successful applications reported are joining and welding polymer and polymer composites (Siores and Groombridge, 1995; Prasad *et al.*, 1998; Potente *et al.*, 2003; Benitez *et al.*, 2007), processing of thermoplastics (Ku *et al.*, 2001; Ku et al., 2003; Makeiff and Huber, 2006; Wang *et al.*, 2007), vulcanizing rubber (Krieqer, 1992; Martin *et al.*, 2002; Pojanavaraphan and Magaraphan, 2008), polymerization (Jacob *et al.*, 1995) and the preparation of polymer foams (Lye *et al.*, 1996; Wongsuban *et al.*, 2003).